

WORKFLOW FOR BIOPRINTING OF CELL-LADEN BIOINK

Sebastian Allig, Margot Mayer and Christiane Thielemann

BioMEMS Lab, Faculty of Engineering, University of Applied Sciences Aschaffenburg, Germany

Abstract

Applying technologies of additive manufacturing to the field of tissue engineering created a pioneering new approach to model complex cell systems artificially. Regarding its huge potential, bioprinting is still in its infancies and many questions are still unanswered. To address this issue, an extrusion-based bioprinting (EBB) process was used to deposit human embryonic kidney (HEK) cells in a defined pattern. It was shown that the bioprinted construct featured a high degree in viability reaching up to 77% 10 days after printing (DAP). This work displays a proof of principle for a controlled cell formation which shall later be applied to *in vitro* drug screening tests using various types of cells.

Keywords

Extrusion-based bioprinting, bioink, tissue engineering, *in vitro* cell systems

Introduction

An alternative to animal experiments are *in vitro* cell models. Therefore, pharmacological treatments can be applied to cells cultured in petri dishes or on a read-out device like f.e. a microelectrode array (MEA)-chip. While most *in vitro* cell models are defined by self-assembly of the cells, researchers are attempting to engineer specified cell patterns. Up to now, multiple methods to engineer cell network are available in literature to make those tests repeatable and controllable. Some interesting approaches are presented briefly at this point.

Firstly, surfaces are modified chemically with molecules like proteins or polylysines to generate a pattern in terms of cell adherent and cell repellent [1, 2]. Those can be added spatially by microcontact printing [3]. The resulting coatings influence cell placement as well as cell outgrowth. Secondly, microstructures can be used to entrap cells in multiple wells connected by microtunnels. Those tunnels route appearing cell proliferation over time to form the desired network [4]. A combination of the afore mentioned approaches is the application of a cell suspension flowing through a microfluidic device which entraps single cells at specified positions [5]. All these laborious approaches aim to bring control and consistency into the formation of cell networks.

In contrast, the field of tissue engineering employs a revolutionary method adapted from rapid prototyping to create cell constructs by additive manufacturing. When speaking about additive manufacturing in a biological context, this technique is commonly termed bioprinting [6]. This method describes layer-by-layer

deposition of a bioink to form a defined construct of cells or at least a scaffold. Ozbolat et al. set up two categories of bioinks [7]. On the one hand, there are scaffold-based bioinks, where cells are embedded in exogenous material which is referred to as cell-laden. On the other hand, scaffold-free bioinks feature processes based on multiple engineered neotissues, which are then combined to larger scale tissues. An extended classification of bioink material is presented in Fig. 1.

Bioprinting not only increases reproducibility of experiments but enables also a third dimension to reach a next level of cell modellings in terms of biomimicry.

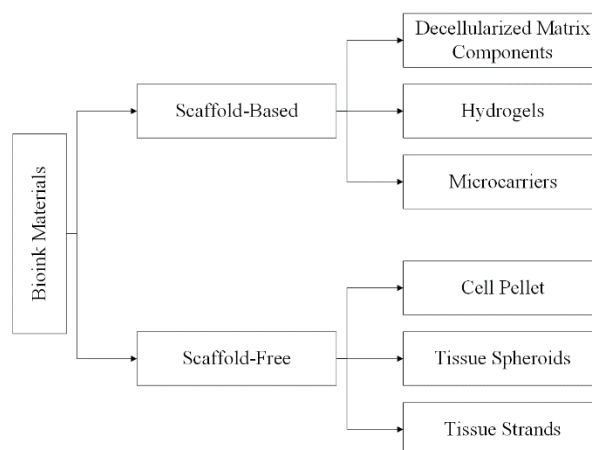


Fig. 1: Classification of bioink materials (figure adapted from Ozbolat et al. [7]).

Since this technology is still emerging, it is of high importance to put forth and establish new methodologies of preparation, printing, culturing and evaluation. In

short, bioprinting involves the following steps to create an artificial tissue: Firstly, a 3D model of the desired tissue is created either by means of computer aided design software or reverse engineering methods such as a laser scanner, magnetic resonance tomography or coherence tomography. Based on this model, a so-called slicer is used to generate the machine code for the bioprinter. In a next step, the bioprinter prints the structure in accordance to the machine code. After printing, post-processing, which mainly depends on the printed material and its purpose, is performed. Finally, the artificial tissue is cultured under appropriate conditions.

When speaking about current challenges in the field of bioprinting, especially vascularization is limiting long-term cultivation. This issue is preventing scientists from creating complex tissues and organs. In this context, there is a big need for nano-scale scaffolds featuring a high degree of biocompatibility as well as biomimicry and thus various advanced bioinks were developed by research and even industry. Those bioinks must feature cytocompatible properties tailored for various cell types and applications individually to maximize cell growth and differentiation capabilities [8].

In this study, human embryonic kidney (HEK) cells were printed in combination with a bioink (Cellink, Goteborg, Sweden) and cell viability was investigated with fluorescence staining. HEK cells have been widely used in cell biology research because of their reliable growth and are here employed as an exemplary cell culture. Thus the aim of this work was the development of a workflow for a bioprinting process including substrate and bioink preparation, tissue construction and viability determination. Thereby, possible challenges and improvement proposals are presented.

Materials and Methods

Substrate preparation

Structures were printed on CELLSTAR™ multiwell plates (Greiner Bio-One, Kremsmünster, Austria) made of polystyrene. For coating, 2 ml of Polyethyleneimine (PEI, 0.1% in boric acid buffer) was applied to each well and incubated for one hour at room temperature. Afterwards, PEI was aspirated, the well rinsed 4 times with deionized (DI) water and air-dried overnight. On the next day, laminin (20 µg/ml in PBS) was applied to the well and incubated for 1 hour at 37°C. Immediately before addition of cells, excess laminin was aspirated.

Bioink preparation

In this study, HEK cells were used. HEK cells were grown in DMEM/Ham's F-12 with stable glutamin (Biochrom GmbH, Berlin, Germany) containing 10% FCS and 1% penstrep at 37°C in a humidity-controlled

incubator with 5% CO₂. Before printing, the culture medium was aspirated and cells washed with 1,5 ml of phosphate buffered saline (PBS). Then, HEK cells were dissociated using 1.5 ml of trypsin/EDTA at 37°C for 6 min. The reaction is stopped with cell culture medium. A cell density of 20x10⁷ cells/ml was determined using a Neubauer cell counting chamber to obtain a final cell concentration of 20x10⁶ cells/ml within the bioink blend. This number was reported to be suitable for bioprinting by Puelacher et al [9].

In this approach, the commercially available Cellink Bioink RGD (Cellink) was used and handled in accordance to its datasheet. In short, this hydrogel based bioink consists of water, alginate, nanofibrillated cellulose (NFC) and RGD peptides. Firstly, alginate is a naturally derived hydrogel and it is known as an artificial extracellular matrix material and thus suitable for bioinks [10]. Secondly, NFC is an additive to increase the shear-thinning behavior and consequently printability of the bioink [11]. Furthermore, NFC ameliorates cell growth within the bioink matrix since cells prefer to grow along micro- or even nanofibers [12]. Thirdly, the peptide RGD of the protein fibronectin increases cell adhesion and thus cell growth [13].

A Cellmixer (Cellink) enables a homogenous distribution of cells inside the bioink. Therefore, 3 ml of bioink is loaded in a 3 ml syringe, while 0.3 ml of the cell suspension is loaded in a 1 ml one, resulting in a 1:10 mixing ratio. Both syringes are adjusted in the dispensing unit, where applying gentle pressure mixes both volumes and dispenses into a 3 cc cartridge. This cartridge is then inserted into the bioprinter.

Bioprinting

The drawing suite BioCAD™ (regenHU, Villaz-Saint-Pierre, Switzerland) is an easy to use tool to generate machine code based on a previously defined pattern. This code includes the tool path as well as most of the printing parameters. Since BioCAD™ supports standard multiwell plates, the pattern was printed in each of the six wells in one job. The printing speed along x and y axis was set to 400 mm/min and the meandering pattern, often used in literature, extends over an area of 15 mm × 15 mm. The interline distance of the parallel lines was set to 2 mm which therefore defines the limit of the extruded line width.

The cell-laden bioink was extruded pneumatically through a 25 gauge precision needle (250 µm inner diameter) by means of the bioprinter 3D Discovery™ (regenHU) at different pressure levels (100 kPa, 75 kPa, 60 kPa and 50 kPa). How extrusion-based bioprinting (EBB) works is depicted in Fig. 2. The resulting strand width varies depending on pressure level as nozzle diameter and printing speed are constant. The viscosity of the material to be printed and the desired structure are prevailing when it comes to finding suitable printing parameters.

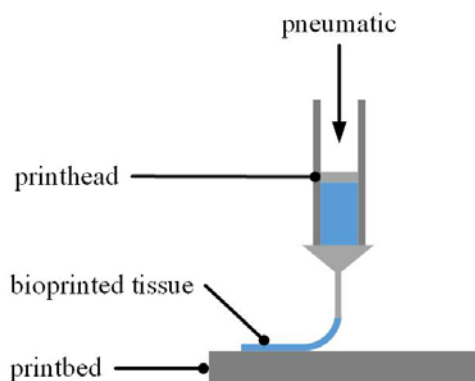


Fig. 2: Schematic of EBB process. The printhead is movable in x/y and z axis along the given toolpath. The bioink is loaded into the printhead by means of a cartridge. The print bed can be equipped with any kind of substrates such as multiwell plates or a MEA chip.

Post processing and cell cultivation

Past printing, some bioinks need an increase of stiffness to provide shape fidelity. This alginate-based ink can be crosslinked by applying 0.5 ml of calcium chloride solution (Cellink) for 5 min once the desired structure was printed. How calcium cations settle in between alginate chains and thus increasing viscosity of the material is described by the *egg-box model*; a detailed explanation can be found elsewhere [14]. After the crosslinking step, the well is filled up with 5 ml of cell culture medium.

Evaluation using transmitted light and fluorescence microscopy

The effect of the printing process on HEK cells was investigated using a live/dead assay based on fluorescent dyes. Therefore, CellTracker™ Green CMFDA (Thermo Fisher Scientific, Waltham, USA) was employed to label viable cells while DAPI tagged nuclei of dead ones. To track the cells, 2 ml of DMEM/Ham's F12 containing CellTracker™ (1 μ M) and DAPI (1 μ g/ml) were applied to each well and incubated for 60 min at 37°C. Afterwards, staining solution was removed, and the well was washed with new medium to remove left-over of the fluorophores. In a next step, transmitted-light picture in addition to a 300 μ m high stack of 30 greyscale pictures for each fluorescence channel were recorded using the Nikon Eclipse Ti (Nikon, Tokyo, Japan) inverted microscope. This stack of pictures is necessary since cells are arranged in a 3D way within the scaffold and thus employing different levels of focus. The extended depth of focus software plug-in for NIS Elements (Nikon, Tokyo, Japan) was taken in account to create a focused image from the previously recorded sequence of Z-stack images.

Data analysis

Recorded images were processed with ImageJ (National Institutes of Health, Bethesda, USA). To assess the degree of cell viability, the number of viable and dead cells respectively were determined using the particle analyzing function of the Fiji software package. Afterwards, the number of viable cells was set in proportion to the total amount of detected cells.

Results

Adhesion improvement using PEI and laminin coating

First experiments with HEK cells showed that the bioprinted structure detached from the bottom of the well once either crosslinking solution or medium was present (Fig. 3a). To address this issue, further experiments were conducted at which the surface was coated with PEI and laminin, see section *Substrate Preparation*. The results showed that cell detachment was prevented and that used coatings guarantee adhesion between artificial tissue and surface as shown in Fig. 3b.

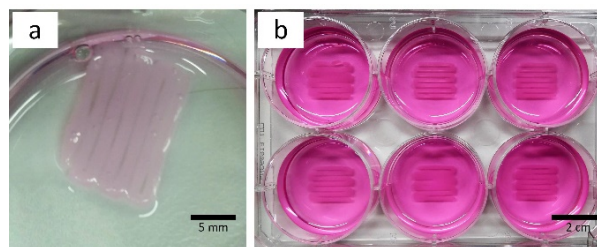


Fig. 3: Printed meandering structure detached from surface without PEI and laminin coating (a, culture medium was removed) and same structure on coated surface to guarantee tissue adhesion (b, culture medium present).

Influence of extrusion pressure on printability

A study of the printed constructs provided insights into the influence of the applied extrusion pressure on the printing results (Fig. 4). A reduction in strand width was noticeable with a descending pressure level at constant printing speed and nozzle dimensions. Based on those observations, it is drawn that structures printed with 75 kPa and 60 kPa showed best printability in relation of the desired structure (Fig. 4b and 4c). In contrast, 100 kPa extrusion pressure tended to create overlapping strands (Fig. 4a) while 50 kPa employed defects in the pattern (Fig. 4d). Relation between strand width and extrusion pressure is further covered in the discussion section.

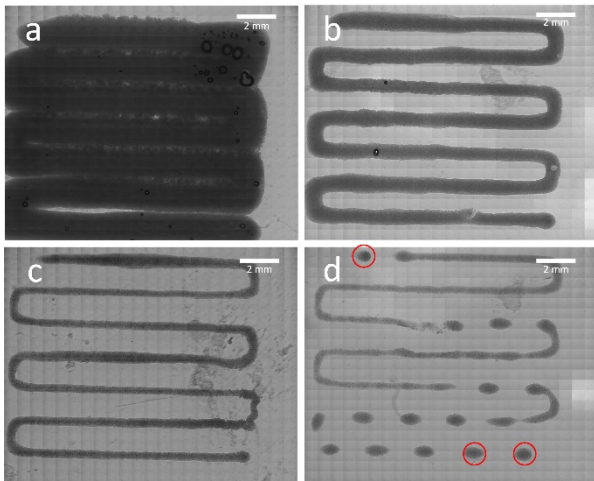


Fig. 4: Analysis of printability. Patterns were printed with 100 kPa (a), 75 kPa (b), 60 kPa (c) and 50 kPa (d). Red circles indicating spots within the scaffold which were observed in terms of cell viability.

The width of a printed strand was measured at 5 randomly selected positions throughout all the pressure levels.

Cell viability

To obtain information about the effect of the EBB process on the HEK cells, the cell-laden scaffolds printed with 50 kPa were analyzed at 0 DAP, 3 DAP, 6 DAP and 10 DAP.

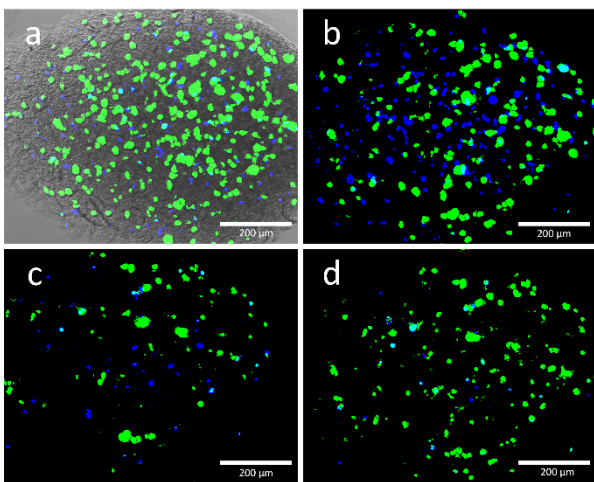


Fig. 5: Viable (green) and dead (blue) HEK cells were found in the printed structure. Each image shows the same position of a scaffold printed with 50 kPa. Images were taken at 0 DAP, 3 DAP, 6 DAP and 10 DAP and they are matching the alphabetic order of the figures. Image a) was merged with a transmitted light image to get an impression at the scaffold.

First of all, a homogeneous cell distribution was observed after loading the Cellink bioink with HEK

cells and bioprinting the cell structures. This indicated a successful mixing process and capability of this bioink to hold the cells in suspension as it is shown Fig. 5.

In addition, it was confirmed that the Cellmixer device offers a cell-laden bioink with almost no air bubbles. Mixing without trapping air is crucial since even small volumes of air trapped in the mixed bioink are compressed during material extrusion and thus influences printing parameters significantly.

Based on the live/dead staining, cell viability post-bioprinting was examined at multiple days. Evaluation of three selected spots within the scaffold printed with 50 kPa is presented in Fig. 6. The 50 kPa sample was chosen because it is likely to feature highest degree of cell viability due to its limited amount of present shear forces. This assumption could be confirmed by further experiments, which are not presented in this work. Notably, the degree of viability is at 83% after printing and further decreasing at 3 DAP due to cell death induced by the printing process. Afterwards, cell viability is increasing at 6 and 10 DAP indicating proliferation of cells that survives printing process.

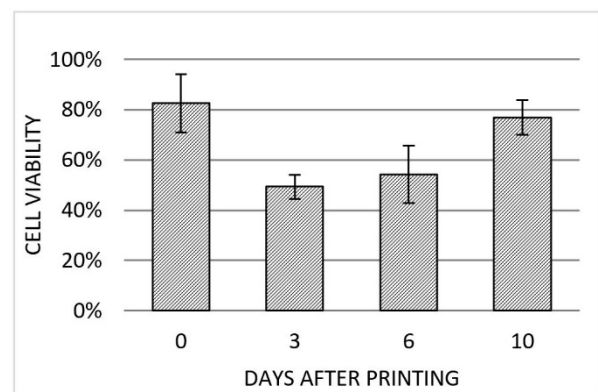


Fig. 6: Cell viability detected right after printing (0 DAP), 3 DAP, 6 DAP and 10 DAP. At each point in time the same three regions of the same scaffold (50 kPa) were investigated. Error bars indicating standard deviation of each data set ($n=3$).

Discussion

One of the hurdles at bioprinting is guaranteeing adherence between printed biomaterial and substrate. When the bioink is brought in contact with culture medium, it swells since hydrogels tend to take up a great amount of fluid [15]. This is leading to an increased porosity due to rearrangement of molecules, which results in a detachment from the substrate. Therefore, it was intended to establish a substrate coating for bottom of multiwell plates to increase the adhesion of the construct. The establishment of a PEI and laminin coating, which has already been reported by Mayer et al. [16], solved this issue and guaranteed

adherence even after several days in cell culture medium.

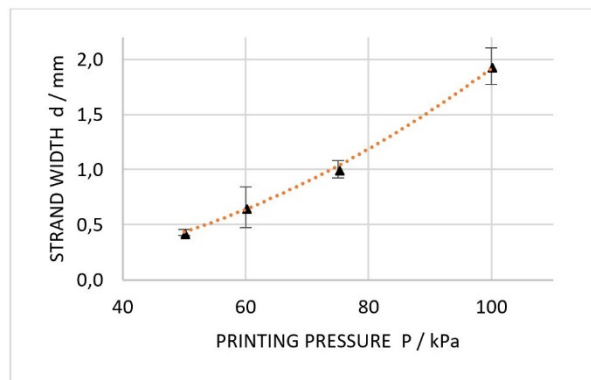


Fig. 7. Dimension analysis of printed strands at extrusion pressures of 50 kPa, 60 kPa, 75 kPa and 100 kPa. Error bars are representing standard deviation of each data point ($n=5$). Orange curve is indicating a square trendline.

Results are plotted in Fig. 7, which are underlined by the findings of Suntornnond et al. [17], who already gave detailed insight into process parameters of EBB. Based on that work, two main relations were derived:

$$d \propto D^2 \sqrt{P} \quad (1)$$

$$d \propto D^2 \sqrt{\frac{1}{v}} \quad (2)$$

where d is the printed strand width, also called resolution, D is the diameter of the nozzle, P is the applied pressure and v is the printing speed along x/y axis.

According to equation (1) (in the slightly modified form $d^2 \propto P$) we find that the applied extrusion pressure is proportional to the square of the resulting strand. The fitting curve in Fig. 7 affirms this relation.

Furthermore, equations (1) and (2) suggest that decreasingly applied pressure as well as increasingly printing speed results in smaller constructs. At same, cell viability is on the increase reducing the applied pressure since cells are consequently be exposed to less mechanical stress. Notably, a small change in nozzle diameter has a large influence on resolution, but nozzle diameter is reciprocal to appearing shear forces and thus decreasing cell viability. Since EBB is similar to fused-deposition modelling (FDM), a 3D printing method for solid material, knowledge in that field can be applied to EBB as well. In practice, this means that according to a thumb rule for FDM, it is recommended that nozzle diameter is maximum the half of the smallest feature size to be printed [18]. Therefore, it is important to choose the nozzle dimensions appropriate to the desired construct in a first place. Moreover, the embedded cells must be significantly smaller than the nozzle, which is

crucial especially in case aggregated cell spheroids, e.g. neurospheres, are present in the bioink. In this study, the cells were 10 to 20 μm in diameter resulting in a very high nozzle to cell ratio. Once a nozzle diameter is chosen, printing of straight lines will help to find extrusion pressure as well as printing speed matching the rheological properties of the formulated bioink [19].

Using the mixing device of Cellink, HEK cells were homogenously distributed within the Cellink bioink. This result was drawn based on the homogenously spread cells in the scaffold seen in Fig. 5. Since no design imperfections were found throughout all the samples printed with 100 kPa, 75 kPa and 60 kPa, no significant amount of air was brought in while mixing. Due to insufficient printing pressure, skips were only found at samples printed with 50 kPa.

Cell viability was quantified by fluorescence microscopy. However, the enumeration of viable and dead cells showed that viability was decreasing right after printing. This suggests that the present shear forces still had a significant influence on the prosperity of the cells. Blaeser et al. already proved that reducing shear stress while bioprinting is crucial to minimize cell loss [20]. In the same study, it was shown that if shear stress is kept below a specific threshold, the bioprinting process will not affect cell viability and proliferation capacity any further. This finding can be applied to the current experimental setup by reducing pressure and printing speed simultaneously. However, it was demonstrated that the used bioink scaffold enabled diffusion of nutrients and gas because cells were cultured within the bioink up to 10 DAP and viability even rised to 77% during this period. To sum it up, the following bioprinting design steps can be followed to reach high experimental outcome in terms of cell viability as well as pattern complexity and quality:

1. Choice of nozzle diameter according to cell diameter
2. Creation of pattern printable with choosen nozzle
3. Selection of low level printing pressure
4. Parameter sweep for printing speed to find needed value for the desired pattern

Conclusion and Outlook

Using bioprinting to engineer well-defined cell patterns in few steps was considered as an alternative to time intense formation methods, which has already been presented by literature. In this context, a meandering structure of HEK cells embedded in a commercially available bioink was created by means of a bioprinter. A viability of 77% was detected 10 DAP within the printed scaffold. This high degree of cell viability on 10 DAP is a promising base for long-term cultivation of 3D tissues built with a bioprinter. The gathered knowledge including the proposed workflow will be

applied to future experiments with more specific cell cultures, namely the printing of neuronal cells. Further, the presented bottom-up approach shall be integrated within the MEA-chip technology enabling functional recording and basic research in neuroscience like the treatment of degenerative diseases or understanding of connectivity.

Another approach worth considering is the application of droplet-based-bioprinting techniques instead of extrusion-based ones. A direct comparison of both methods with same bioink and same cell type is still missing in literature.

References

- [1] Clark, P., et al.: *Growth cone guidance and neuron morphology on micropatterned laminin surfaces*. Journal of cell science, 1993, 105(1): 202–212.
- [2] Jungblut, M., et al.: *Triangular neuronal networks on microelectrode arrays: an approach to improve the properties of low-density networks for extracellular recording*. Biomedical microdevices, 2009, 11(6): 1269–1278.
- [3] Ruiz, S. A., et al.: *Microcontact printing: A tool to pattern*. Soft Matter, 2007, 3(2): 168–177.
- [4] Pan, L., et al.: *An in vitro method to manipulate the direction and functional strength between neural populations*. Frontiers in neural circuits, 2015, 9(32).
- [5] Krumpholz, K., et al.: *A microfluidic device for selective positioning of invertebrate neurons*. 9th int. meeting on substrate-integrated microelectrode arrays, 2014.
- [6] Jones, N.: *Science in three dimensions: the print revolution*. Nature, 2012, 487(7405): 22–23.
- [7] Ozbolat, I. T.: *3D Bioprinting: Fundamentals, Principles and Applications*. 1st ed. Academic Press, 2017.
- [8] Husain, S. R., et al.: *Current status and challenges of three-dimensional modeling and printing of tissues and organs*. Tissue engineering: part A, 2017, 23(11–12).
- [9] Puelacher, W. C., et al.: *Tissue-engineered growth of cartilage: the effect of varying the concentration of chondrocytes seeded onto synthetic polymer matrices*. International journal of oral and maxillofacial surgery, 1994, 23(1): 49–53.
- [10] Rowley, J. A.: *Alginate hydrogels as synthetic extracellular matrix materials*. Biomaterials, 1999, 20(1): 45–53.
- [11] Martinez, H., et al.: *3D bioprinting of human chondrocyte-laden nanocellulose hydrogels for patient-specific auricular cartilage regeneration*. Bioprinting, 2016, 1(2): 22–35.
- [12] Möller, T., et al.: *In vivo chondrogenesis in 3d bioprinted human cell-laden hydrogel constructs*. Plastic and reconstructive surgery global open, 2017, 5(2): 1227.
- [13] Prowse, A. B. J., et al.: *Stem cell integrins: implications for ex-vivo culture and cellular therapies*. Stem cell research, 2011, 6(1): 1–12.
- [14] Grant, G. T., et al.: *Biological interactions between polysaccharides and divalent cations: The egg-box model*. FEBS Letters, 1973, 32(1): 195–198.
- [15] Ahmed, E. M., et al.: *Hydrogel: preparation, characterization, and applications: a review*. Journal of advanced research, 2015, 6(2): 105–121.
- [16] Mayer, M., et al.: *Electrophysiological investigation of human embryonic stem cell derived neurospheres using a novel spike detection algorithm*. Biosensors and bioelectronics, 2018, 100: 462–468.
- [17] Suntornnond, R., et al.: *A mathematical model on the resolution of extrusion bioprinting for the development of new bioinks*. Materials, 2016, 9(9): 756.
- [18] Gibson, I., et al.: *Additive manufacturing technologies: 3D printing, rapid prototyping and direct digital manufacturing*. Springer, New York, 2015, 2nd edition.
- [19] He, Y., et al.: *Research on the printability of hydrogels in 3D bioprinting*. Scientific Reports, 2016, 6:29977.
- [20] Blaeser, A., et al.: *Controlling shear stress in 3D bioprinting is a key factor to balance printing resolution and stem cell integrity*. Advanced healthcare materials, 2016, 5(3): 326–333.

Sebastian Allig, B.Eng.
BioMEMS Laboratory
Faculty of Engineering
University of Applied Sciences Aschaffenburg
Würzburger Str. 45, 63743 Aschaffenburg
Germany

E-mail: biomems@h-ab.de